On the Cover of the Rolling Stone*

Adrian Dumitrescu† Csaba D. Tóth‡

Abstract

We construct a convex polytope of unit diameter that when placed on a horizontal surface on one of its faces, it repeatedly rolls over from one face to another until it comes to rest on some face, far away from its start position: that is, the horizontal distance between the footprints of the start and final faces can be larger than any given threshold. According to the laws of physics, the vertical distance between the center of mass of the polytope and the horizontal surface continuously decreases throughout the entire motion. The speed of the motion is irrelevant. Specifically, if the polytope is manually stopped after each tumble, the motion resumes when released (unless it stands on the final stable face).

Moreover, such a polytope can be realized so that (i) it has a unique stable face, and (ii) it is an arbitrary close approximation of a unit ball. As such, this construction gives a positive answer to a question raised by Conway (1969).

The arbitrarily large rolling distance property investigated here for the first time raises intriguing questions and opens new avenues for future research.

Keywords: perpetuum mobile, rolling distance, unistable polytope, center of mass, laws of physics.

1 Introduction

Oh ye seekers after perpetual motion,
how many vain chimeras have you pursued?
Go and take your place with the alchemists.
— Leonardo da Vinci (1494)

The history of perpetual motion machines dates back to the Middle Ages. The Encyclopaedia Britannica entry dedicated to *Perpetual Motion* reads: "Perpetual motion, although impossible to produce, has fascinated both inventors and the general public for hundreds of years. The enormous appeal of perpetual motion resides in the promise of a virtually free and limitless source of power. The fact that perpetual-motion machines cannot work because they violate the laws of thermodynamics has not discouraged inventors and hucksters from attempting to break, circumvent, or ignore those laws." Indeed, this fact did not discourage us either, and the current paper can be viewed as yet another attempt. It offers a good approximation of such a device in the sense that the range of the motion can be arbitrarily large and prescribed beforehand.

Imagine a convex polyhedron standing on a horizontal surface in Euclidean 3-space. The body is stable on the facet that it stands on if and only if its center of mass projects vertically in the interior of that facet. For example, a tall prism that leans like the Tower of Pisa is unstable (a suggestive example offered by Dawson et al. [10]). Obviously, Platonic solids of uniform density are, by symmetry, stable on all their facets. Note however that the *uniform density* is a key assumption: If we place a regular octahedron on a facet (base) and concentrate its mass in one of the vertices whose projections lie outside of the base facet, the octahedron rolls onto an adjacent facet.

A convex polytope will roll from one facet to another only if it thereby monotonically lowers its center of mass; it therefore follows that no polytope can ever roll back to a facet from which it has rolled away, and so every polytope has at least one facet upon which it is stable. A polytope that is stable upon only one of its facets is called *unistable* (or sometimes *monostatic*, *unistatic*, or *monostable*); see, e.g., [10, 11].

Clearly, if the body is allowed to have nonuniform (but positive) density, the center of mass may be anywhere in the interior of the body. As reported in [9], Conway constructed a tetrahedron in $\mathbb{R}^3$ which, with a suitably positioned center of mass, is stable only on one facet. Moreover, this tetrahedron, when placed on one of its facets, can roll onto each of its 4 facets until it reaches a stable position. Conway [16] also constructed a unistable convex polytope (a truncated cylinder of uniform density) with 19 faces; the cross-section of the cylinder is a 2D convex polygon that is unistable with nonuniform density. The cylinder

*Title inspired by the song *The Cover of "Rolling Stone"* by *Dr. Hook & The Medicine Show*, 1972.

†Department of Computer Science, University of Wisconsin–Milwaukee, WI, USA.

‡Department of Mathematics, California State University Northridge, Los Angeles, CA; and Department of Computer Science, Tufts University, Medford, MA, USA. Research by this author was supported in part by the NSF awards CCF-1422311, CCF-1423615, and DMS-1800734.

is truncated by slanted planes to move the center of mass to the desired position. Bezdek [3] reduced the number of faces to 18, while the current record, 14, is obtained by computer search [24]. See [12, Sec. 4] for combinatorial properties of small unistable polytopes in $\mathbb{R}^3$. Related work regarding unistability of polytopes include [8, 17]; see also [7, Sec. B12].

This definition of stability may be extended, somewhat less physically, to polytopes in other dimensions, including the plane. Conway showed [6] that in the plane, no convex polygon of uniform density is unistable, and that in 3-space no tetrahedron of uniform density is unistable. Heppes [18] constructed a tetrahedron which, placed upon the appropriate face, rolls twice before reaching one of its two stable faces. It thus tours all of its unstable faces before reaching equilibrium. Heppes asked in how few dimensions, if any, a full-dimensional simplex could be unistable. Dawson et al. [10] constructed a unistable simplex in $\mathbb{R}^{10}$ and showed that no such simplex exists in $\mathbb{R}^7$; computational evidence suggests that no such simplex exists in $\mathbb{R}^8$ and $\mathbb{R}^9$. Dawson et al. [10] also exhibit a unistable simplex in $\mathbb{R}^{11}$ that sequentially rolls through all 12 facets.

Static equilibria of convex bodies (allowing smooth surfaces) have also been studied; stable and unstable equilibria are related to sinks and sources in the gradient vector field characterizing the surface. The total number of equilibria is governed by the Poincaré-Hopf Theorem [2]. For example, a polytope standing on a vertex may be at equilibrium, but this equilibrium is unstable. Várkonyi and Domokos [26], settling a conjecture due to Arnold (1995), constructed a smooth convex body (called *gömböc*) with a unique stable and a unique unstable equilibrium. Their discovery has lead to a systematic study of the topological properties of stable and unstable points [13]. However, it is not obvious how to approximate a smooth convex body by a polyhedron with the same stability: Domokos et al. [14] show that uniformly random discretization may introduce additional stable equilibria.

Although our focus in this paper falls along these lines, it is headed in a different direction.

Question 1. *How far can a polytope of unit diameter roll when placed on a horizontal surface?*

Question 2. *For every sufficiently large n, does there exist a polytope with n facets, and an ordering of the facets, $f_1, f_2, \ldots, f_n$, so that if P is placed upon f_i, it will roll through facets $f_{i+1}, \ldots, f_n$ until resting on its unique stable facet f_n?*

The distance traveled by a rolling polytope could be measured in ways such as: (i) the length of the trajectory of the projection of some reference point of the polytope (for instance, the center of mass) onto the horizontal plane, or simply as (ii) the distance between the footprints of the start and final faces in the horizontal plane. For convenience, we stick to the latter measure that we find more intuitive as well as serving our intent.

Notation and terminology. For brevity, a convex polyhedron of uniform density is called *uniform*. For a convex polytope P in $\mathbb{R}^d$, let $\xi(P)$ denote the center of mass. The *perimeter* of P, denoted $\mathrm{per}(P)$, is the sum of the edge lengths of P. The boundary of P is denoted by ∂P.

For a line segment s, let $\ell(s)$ denote the line containing s. For two points $p, q \in \mathbb{R}^d$, let $d(p, q)$, or sometimes $|pq|$, denote the Euclidean distance between them; while the length of a rectifiable curve C is denoted by $\mathrm{len}(C)$. For two sets of points $A, B \subset \mathbb{R}^d$, their distance is $d(A, B) = \inf\{d(a, b) \mid a \in A, b \in B\}$. A hyperplane H is given by the linear equation $H = \{x \in \mathbb{R}^d : a \cdot x = b\}$, where $a \in \mathbb{R}^d$ and $b \in \mathbb{R}$. The closed ball of radius r in $\mathbb{R}^d$ centered at point $z = (z_1, \ldots, z_d)$ is $B_d(z, r) = \{x \in \mathbb{R}^d \ : \ d(z, x) \le r\}$. A *unit ball* is a ball of unit radius in $\mathbb{R}^d$.

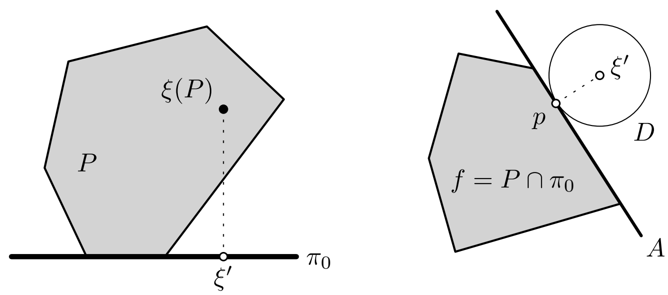

Figure 1: Left: A convex polygon (or polytope) P, its center of mass $\xi(P)$, and its projection ξ' to the horizontal hyperplane π_0. Right: A polytope in $\mathbb{R}^d$ stands on a face $f = P \cap \pi_0$, its center of mass vertically projects to ξ' in the exterior of f, and P rolls about the axis A.

Rules of motion. Consider a convex body P in $\mathbb{R}^d$, standing on a horizontal hyperplane π_0. By the laws of physics, the potential energy of P equals to mgh, where m is the mass of P and h denotes the vertical distance from $\xi(P)$ to π_0. The body P rolls without slipping only if the height of $\xi(P)$ strictly decreases. By Gauss' principle of least constraint [15], the direction of the motion maximizes the rate of descent, i.e., minimizes the slope of the direction vector of the trajectory of $\xi(P)$. In particular, a polytope P standing on a face f rolls (to another face) if and only if the vertical projection onto π_0 of the center of mass of P, $\xi(P)$, lies in the exterior of f; see Fig. 1 (left).

Denote this projection point by ξ'. Let D be the largest ball in the horizontal hyperplane π_0 centered at ξ' whose interior is disjoint from f. Then ∂D intersects f in a single point p. The steepest descent of $\xi(P)$ occurs when P rotates around the $(d-2)$-dimensional axis $A \subset \pi_0$ tangent to D at point p; see Fig. 1 (right). During the rotation, the face $A \cap P$ remains fixed, and the rotation stops when $P \cap \pi_0$ becomes a higher-dimensional face. In particular in $\mathbb{R}^3$, if $A \cap P$ is an edge e, then P rotates about e to an adjacent face; and if $A \cap P$ is a vertex, then P rotates about A until P "lands" on a facet or an edge. The polytopes we construct in Sections 3–4 always roll around edges if initially placed on an unstable face.

Note that the rolling motion is governed by discrete geometry alone. In particular, it does not take the *moment of inertia* into account, e.g., as if the convex polytope were moving in a fluid of high viscosity. The rolling motion of a smooth convex body with moment of inertia is a problem in classical dynamics that can be characterized by differential equations. For example, Chaplygin [5] described the motion of a nonuniform ball on a horizontal plane in 1903. We do not pursue that direction here.

Discussion. In the plane, the distance referred to in Question 1 is clearly bounded: as noted above, a convex polygon P stands on each of its faces at most once during a rolling motion, consequently the distance traveled cannot exceed the perimeter of P, which is at most π by the isodiametric inequality. Somewhat surprisingly, the answer to Question 1 in 3-space is "As far as we like." Therefore, such a polytope is in some sense a good approximation of a *perpetuum mobile*. The precise statement is in our Theorem 3.1 (in Section 3).

A variant of our construction (Theorem 4.1 in Section 4) is related to the following question raised by Conway [16, p. 81], [7, Sec. B12], to which it gives a partial answer: "What is the set of convex bodies uniformly approximable by unistable polyhedra, and does this contain the sphere?"

To formulate our results it is first convenient to strengthen the concept of unistable polytope as follows. We say that the pair $(P, \xi(P))$ of a polytope and its center of mass is *Hamiltonian unistable* if P is unistable and in addition, there exists an ordering of the facets, $f_1, f_2, \ldots, f_n$, so that if P is placed upon f_i, it will roll to face f_{i+1}, for $i = 1, \ldots, n-1$.

Perpetuum mobile approximations. We show several constructions of polytopes as described below. The polytopes in constructions (i)–(iii) need not be uniform, and only the one in (iv) yields a uniform polytope.

(i) For every $\varepsilon > 0$, we construct a Hamiltonian unistable convex polygon P in $\mathbb{R}^2$ that can be placed on a horizontal line upon one of its sides so that it repeatedly rolls over covering a horizontal distance of at least $(1-\varepsilon)\,\mathrm{per}(P)$ (Theorem 2.1 in Section 2).

(ii) For every $L \geq 1$, we construct a Hamiltonian unistable convex polytope of unit diameter in $\mathbb{R}^3$ that can be placed upon one of its facets so that it repeatedly rolls over until it comes to rest on its unique stable face at a distance of at least L from its start position (Theorem 3.1 in Section 3).

(iii) The polytope in Theorem 3.1 can be an arbitrary close approximation of a ball (Theorem 4.1 in Section 4). This gives a partial answer to a 50-year old question raised by Conway [16]; see also [7, Sec. B12].

(iv) For every $L \geq 1$, there exists a *uniform* convex polytope of unit diameter (albeit not necessarily unistable or Hamiltonian) in $\mathbb{R}^3$ that can be placed upon one of its facets so that it repeatedly rolls over covering a horizontal distance of at least L (Theorem 4.2 in Section 4).

1.1 Preliminaries

The proofs of the following lemmas are folklore; refer to Fig. 1.

LEMMA 1.1. *Let P be a convex polytope in $\mathbb{R}^d$ and p any point contained in P. Then there exists a face f of P so that the orthogonal projection of p onto its supporting hyperplane is contained in f.*

Proof. Let $p \in P$, let f_1 be a facet of the polytope whose supporting hyperplane H_1 is closest to p, and let q_1 be the orthogonal projection of p onto H_1. Note that $\mathrm{dist}(p, H_1) = |pq_1|$. If $q_1 \notin f$, then the line segment pq_1 intersects the boundary of P at some point q_2 contained in some facet f_2, which spans a hyperplane H_2. Then we have $\mathrm{dist}(p, H_2) \leq |pq_2| < |pq_1| = \mathrm{dist}(p, H_1)$, a contradiction. □

An alternative argument for the proof (in Physics terms) is as follows. Make p the center of mass of P, that is, $\xi(P) = p$. Let f be a face of the polytope whose supporting hyperplane is closest to $\xi(P)$. Then f must be stable, since rolling to any other face cannot lower the position of $\xi(P)$.

LEMMA 1.2. *Let P be a convex polytope in $\mathbb{R}^d$ (uniform or not). Then P cannot roll forever.*

Proof. Let $\xi = \xi(P)$ denote the center of mass of P. Assume that P can roll forever on a horizontal surface π_0, while the center of mass monotonically gets closer to π_0. Since P has a finite number of facets, some facet f will repeat; that is, there are two time instances $t_1 < t_2$, so that the vertical distance from ξ to π_0 (and f) at time t_2 is smaller than the vertical distance from ξ to π_0 (and f) at time t_1. This completes the proof. ∎

2 The Planar Case

Let B be a convex body in the plane. As noted above, the distance covered (i.e., the distance between the initial and final footprints) cannot exceed the perimeter of B. Therefore, it is convenient to measure the displacement of a convex body relative to its perimeter.

THEOREM 2.1. *For every $\varepsilon > 0$, we can construct a convex polygon P with $O(\varepsilon^{-2})$ vertices that (i) is Hamiltonian unistable and (ii) can be placed on a horizontal line upon one of its sides so that it repeatedly rolls over such that the distance between the initial and the final contact sides on the horizontal line is at least $(1-\varepsilon)\,\mathrm{per}(P)$. (The polytope P need not be uniform.)*

Proof. Consider two concentric circles, C_1 and C_2, of radii $1-a$ and 1 respectively, centered at the origin o. Let D_1 and D_2 denote the corresponding disks. See Fig. 2. Let γ be an open continuous curve in between the two circles, in the form of a spiral and whose parametric equation is:

$$(2.1)\qquad \left(1-\frac{a}{2\pi}\,t\right)(\sin t,-\cos t),\qquad 0\le t\le 2\pi.$$

Let s be the tangent to γ from the point $(0,-1)$; let $t_0 < 2\pi$ be the corresponding value of t at the tangency point. Let $B = B(\gamma)$ be the planar convex body bounded by an initial segment of the spiral γ and by the tangent s.

We will subsequently construct the polygon $P \subset B$. The center of mass of B is the origin and we do *not* assume uniform density. The same assertions will hold true for P. Observe that $D_1 \subset B \subset D_2$, and so $2\pi(1-a) \le \mathrm{per}(B) \le 2\pi$. Consider also the tangent s_1 to C_1 from the point $(0,-1)$, subtending a center-angle β; its length is

$$|s_1| = \sqrt{1-(1-a)^2} = \sqrt{2a-a^2} \le \sqrt{2a}.$$

Since the tangent s is sandwiched between D_1 and D_2, it follows that $|s| \le 2|s_1|$ and thus $|s| \le \sqrt{8a}$. Set $a=\varepsilon^2$. We have

$$\frac{|s|}{\mathrm{per}(B)} \le \frac{\sqrt{8a}}{2\pi(1-a)} = \frac{2\sqrt{2}\varepsilon}{2\pi(1-a)} \le \varepsilon.$$

Consequently, the horizontal distance covered by B when rolling clockwise after being placed upon its first side is

$$\mathrm{per}(B) - |s| = \left(1-\frac{|s|}{\mathrm{per}(B)}\right)\mathrm{per}(B) \ge (1-\varepsilon)\,\mathrm{per}(B).$$

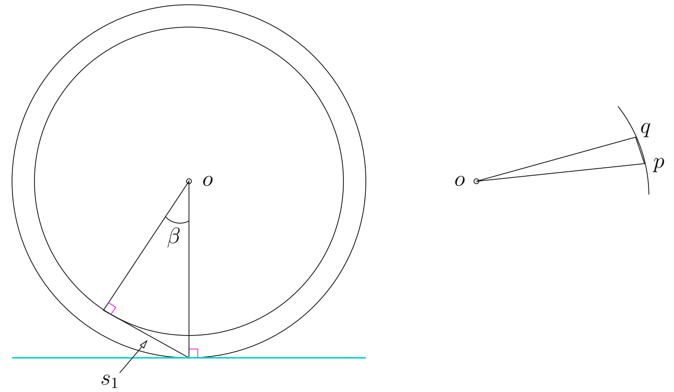

Figure 2: Construction of a unistable polygon P that covers a large distance when it rolls.

We next construct a convex polygon P that mimics the behavior of $B(\gamma)$. We subdivide the boundary of $B(\gamma)$ by choosing a sequence of points that forms the vertex set of P. The first vertex of P is $(0,-1)$. If P rests upon the current side pq, P will roll to the next side of P adjacent to q, provided that the angle $\angle oqp$ of the respective triangle is *obtuse*. Taking this fact into consideration, if vertex p is fixed on γ, the next vertex $q = q(p) \in \gamma$ is chosen as follows. By construction, the distance $|oq|$ is strictly decreasing as q moves away from p, and there is a unique point $q_0 \in \gamma$ such that $\angle oq_0p = \pi/2$. Indeed, the tangent to γ at point p is not orthogonal to the segment op, and so γ enters the interior of the circle with diameter op at p, and it exits at a unique point q_0. As such, the next vertex can be chosen anywhere on the arc pq_0, with q_0 specified as above.

All vertices of P are selected in this way until we reach the point of tangency between s and γ. The last side of P is s; observe that s is the unique stable side of P. Let $x = \angle poq_0$, and put $z = 1-\frac{a}{2\pi}t$; note that $1-a \le z \le 1$. We have

$$(2.2)\qquad \cos x = \frac{1-\frac{a}{2\pi}(t+x)}{1-\frac{a}{2\pi}t} = \frac{z-\frac{a}{2\pi}x}{z} = 1-\frac{ax}{2\pi z}.$$

We may assume without loss of generality that $x \le 1/10$. The well-known Taylor expansion of $\cos x$ around zero yields

(2.3)

$$1-\frac{x^2}{2} \le \cos x \le 1-\frac{x^2}{2}+\frac{x^4}{24} \le 1-\frac{47x^2}{96},\ \text{for } x \le \frac{1}{10}.$$

Applying this estimate in (2.2) further yields that $\frac{a}{\pi} \le x \le \frac{a}{3}$. Recall that we have set $a = 2\varepsilon^2$, thus the length of each side of P can be $\Theta(\varepsilon^2)$; thus P has $O(\varepsilon^{-2})$ sides, as required. ∎

3 The Three-Dimensional Case

In this section we prove the following result.

Theorem 3.1. *For every $L \geq 1$, one can construct a Hamiltonian unistable polytope $P = P(L)$ of unit diameter and with $O(L^6)$ faces in 3-space and specify an ordering $f_1, f_2, \ldots, f_n$, of these faces, so that if P is placed on a horizontal plane π_0 in contact with f_1, the following hold:*

(i) *P successively rolls around the edge $f_i \cap f_{i+1}$, for each $i = 1, 2, \ldots, n-1$.*

(ii) *P comes to rest on the last facet f_n, which is the only stable facet of P.*

(iii) *The horizontal distance between the initial and final contact faces is at least L.*

(The polytope P need not be uniform.)

Proof. We first describe a general construction of a Hamiltonian unistable polytope with center of mass at the origin, and then adjust the parameters to ensure that it has unit diameter and travels a distance at least L away from its initial position. We will assume (for the proof) that L is sufficiently large, i.e., $L \geq L_0$ for a suitable $L_0 \in \mathbb{N}$; then the statements of the theorem automatically hold for any smaller value of L.

General construction. We start with a unit ball B centered at the origin $o = \mathbf{0}$. Let $T \geq 1$ and $\gamma : [0, T] \to \partial B$ be a simple smooth *arc* (open curve) drawn on the surface of B, parameterized by its arc length, that is, its length is T and $|\gamma'(t)| = 1$ for all $t \in [0, T]$. Intuitively, we "scrap off" some neighborhood of γ, while gradually going deeper to the interior of B. We define an arc $\beta : [0, T] \to B$ that follows γ but goes gradually deeper into the interior of B, and then use hyperplanes tangent to $\beta(t)$, for all $t \in [0, T]$ to scrap off a neighborhood of γ.

We continue with the technical details. Let $0 < a \leq 1/10$ be a sufficiently small constant (to be specified later), and let $\beta : [0, T] \to B$ be a curve defined by

$$\beta(t) = \left(1 - \frac{at}{T}\right) \gamma(t) \text{ for } t \in [0, T]. \tag{3.4}$$

Note that $\beta(0) = \gamma(0)$ and $\beta(T) = (1 - a)\gamma(T)$. Also observe that $|\gamma(t)| = |\gamma'(t)| = 1$ for all $t \in [0, T]$; and $0.9 \leq |\beta(t)| \leq 1$ for all $t \in [0, T]$.

For every $t \in [0, T]$, let $\beta'(t)$ be the direction vector of β at t; let $\ell(t)$ be the line incident to $\beta(t)$ and orthogonal to both the direction vector $\beta'(t)$ and the position vector $\beta(t)$. We also define the plane $H(t)$ incident to $\beta(t)$ and parallel to both $\beta'(t)$ and $\ell(t)$; and let $H^+(t)$ be the halfspace bounded by $H(t)$ that contains the origin o. We define the convex body

$$B' = B \cap \left(\bigcap_{t \in [0,T]} H^+(t) \right).$$

We next specify the parameter $a > 0$. For $t = 0$, the line $\ell(0)$ is tangent to B. For $t \in (0, T]$, the line $\ell(t)$ intersects the sphere ∂B at two points at distance $2\sqrt{1 - (1 - at/T)^2}$ apart. The two intersection points trace out two arcs on ∂B, that we denote by γ_{left} and γ_{right}. The plane $H(T)$ intersects ∂B in a circle $C := H(T) \cap \partial B$. Let $a > 0$ be sufficiently small so that both γ_{left} and γ_{right} are simple smooth curves disjoint from each other that intersect the circle C only at the endpoints $\gamma_{\text{left}}(T)$ and $\gamma_{\text{right}}(T)$. By construction, $\beta \subset H^+(t)$ for all $t \in [0, T]$, thus β is a smooth arc on the surface of B'.

As in the proof of Theorem 2.1, the center of mass of B' is the origin o and uniform density is *not* assumed. The same assertions will hold for the polytope P that will be constructed from B'. If B' is placed on a horizontal surface making contact at $\gamma(0) = \beta(0)$, it will start rolling continuously while its center of mass continuously gets closer to the plane π_0, with a contact segment $\gamma_{\text{left}}(t)\gamma_{\text{right}}(t)$ at time $t \in [0, T)$. The body B' stops rolling at time $t = T$, when the contact face is bounded by $\gamma_{\text{left}}(T)\gamma_{\text{right}}(T)$ and a circular segment of C.

Discretization. We construct a polytope P from B' as follows. Let $\delta > 0$ be a sufficiently small parameter (specified below). Consider a subdivision $0 = t_1 < t_2 < \ldots < t_n = T$ of the interval $[0, T]$ such that $t_{i+1} - t_i < \delta$ for $i = 1, \ldots, n-1$. For $i = 1, \ldots, n$, we use the shorthand notation $H_i = H(t_i)$. We can now define P as an intersection of halfspaces as follows.

$$P = \bigcap_{i=1}^{n} H_i^+. \tag{3.5}$$

At this point P is a (possibly unbounded) convex polyhedron; we later choose γ to ensure that P is a (bounded) convex polytope. Note that neither B nor P contains the other body. Since the plane H_i contains the point $\beta(t_j)$ if and only if $i = j$, the polytope P has precisely n faces, one in each plane H_i ($i = 1, \ldots, n$); denote by f_i the face of polytope P contained in H_i.

Lemma 3.1. *If $\delta > 0$ is sufficiently small, as specified in (3.12), then for all $i = 1, \ldots, n-1$,*

(i) *face f_i is unstable, and*

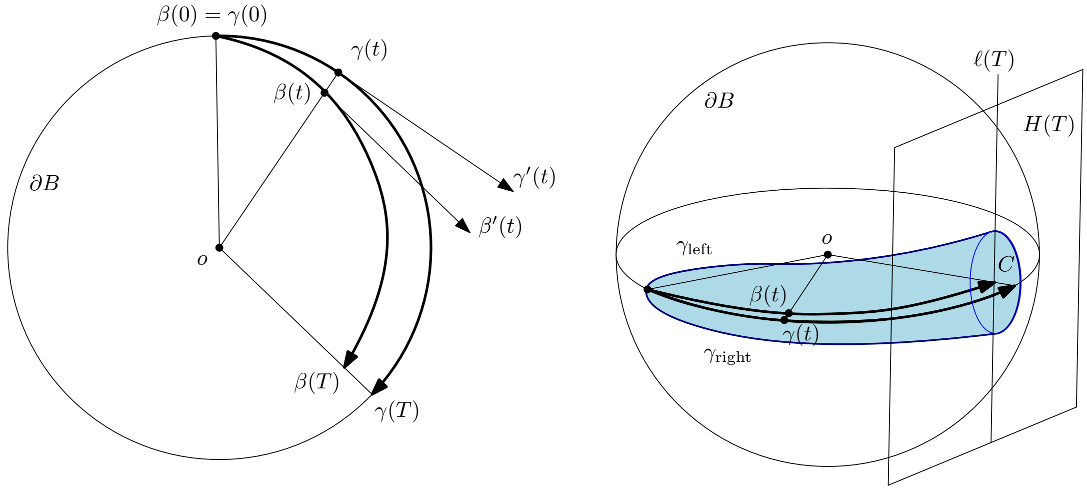

Figure 3: Left: The vectors $\gamma(t)$, $\gamma'(t)$, $\beta(t)$, and $\beta'(t)$ in the special case where γ is a circular arc along the equator. Right: The arcs γ_{left} and γ_{right} traced out by the intersection points $\ell(t) \cap \partial B$; and the circle $C = H(T) \cap \partial B$. The shaded surface has been scrapped off from the ball B.

(ii) *if P stands on face f_i, then it rolls to face f_{i+1}.*

We first summarize our strategy for the proof of Lemma 3.1. Let $h_i \in H_i$ be the orthogonal projection of the origin o to the plane H_i (that is, $oh_i \perp H_i$). We show that $h_i \notin f_i$ for $i = 1, \ldots, n-1$, which establishes part (i). Specifically, we give a lower bound for the distance $|\beta(t_i)h_i|$, and then show that the line $H_i \cap H_{i+1}$ separates points $\beta(t_i)$ and h_i in the plane H_i. Since $f_i \subset H_i$, this implies part (i). For the proof of part (ii), we further show that f_i and f_{i+1} are adjacent (their common edge is contained in $H_i \cap H_{i+1}$). We also show—by eliminating all other options—that if P stands on face f_i, it rolls around this common edge.

Importantly, we give a quantitative upper bound for δ in terms of the second derivative of β; see (3.12). We use this bound later for estimating the number of vertices of P in terms of L. We continue with the details.

Recall that γ is a simple smooth arc on the surface of B. Consequently, its direction vector $\gamma'(t)$ at $t \in [0,T]$ is tangent to ∂B, hence orthogonal to the position vector $\gamma(t)$; see Fig. 3 for an illustration. The direction vector of $\beta(t)$ can be computed as follows:

$$\begin{aligned} \beta'(t) &= [(1-at/T)\gamma(t)]' \\ &= (1-at/T)\gamma'(t) - (a/T)\gamma(t), \end{aligned} \tag{3.6}$$

where $\gamma(t)$ and $\gamma'(t)$ are orthogonal unit vectors. In particular,

$$1-a \le 1-\frac{at}{T} \le |\beta'(t)| \le \left(1-\frac{at}{T}\right)+\frac{a}{T} \le 1+\frac{a}{T}. \tag{3.7}$$

Recall that $T \ge 1$, and consequently we have

$$\tan\angle(\beta'(t),\gamma'(t)) = \frac{(a/T)|\gamma(t)|}{(1-at/T)|\gamma'(t)|} = \frac{a/T}{1-at/T} \ge \frac{a}{T}$$

for all $t \in [0,T]$.

Recall that $\ell(t)$ is orthogonal to both $\beta(t)$ and $\beta'(t)$. Since $\ell(t)$ is parallel to $H(t)$, the orthogonal projection of o to $H(t)$ lies in the plane $\langle\beta(t),\beta'(t)\rangle$. In particular, for $i = 1, \ldots, n-1$, point $h_i \in H_i$ lies in the plane $\langle\beta(t_i),\beta'(t_i)\rangle$. Consider the right triangle $\Delta(\beta(t_i)oh_i)$. Since $\beta(t_i)$ and $\gamma'(t_i)$ are orthogonal, we have

$$\angle\beta(t_i)oh_i = \angle(\beta'(t_i),\gamma'(t_i)) \ge \arctan(a/T).$$

Consequently,

$$\begin{aligned} |h_i - \beta(t_i)| &= |\beta(t_i)| \cdot \sin\angle(\beta'(t_i),\gamma'(t_i))) \\ &\ge |\beta(t_i)| \cdot \sin\left(\arctan(a/T)\right) \\ &> \frac{9}{10} \cdot \frac{a/T}{2} > \frac{a}{3T}. \end{aligned} \tag{3.8}$$

For every $s,t \in [0,T]$, the position $\beta(t)$ can be approximated using Taylor's estimate with Lagrange remainder

$$\beta(t) = \beta(s) + (t-s)\beta'(s) + \frac{\beta''(\xi)}{2}(t-s)^2, \tag{3.9}$$

where $\xi \in [\min\{s,t\},\max\{s,t\}]$. Let

$$M = \max_{\xi\in[0,T]} |\beta''(\xi)|.$$

Then (3.9) yields

$$|\beta(t) - (\beta(s) + (t-s)\beta'(s))| \le \frac{M}{2}(t-s)^2. \tag{3.10}$$

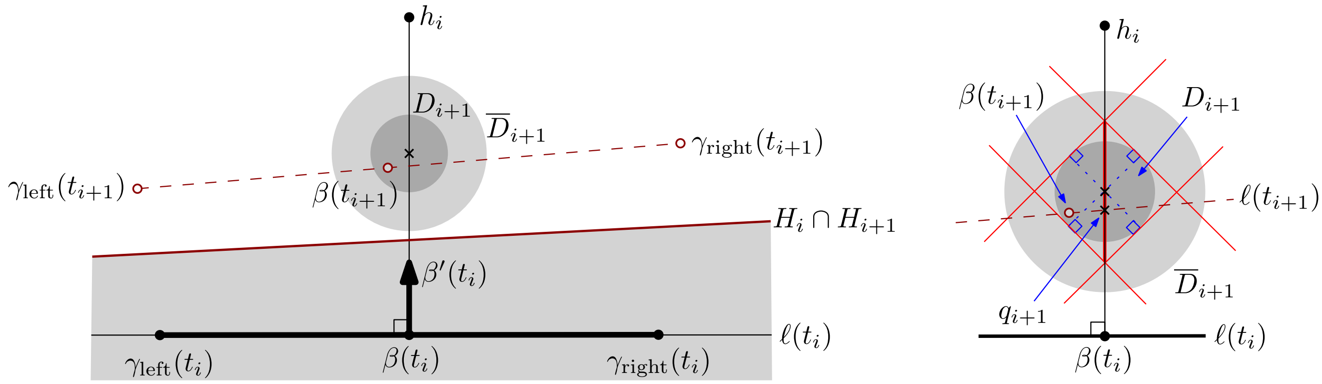

Figure 4: Points $\beta(t_i)$ and h_i, and segment $\gamma_{\rm left}(t_i)\gamma_{\rm right}(t_i)$ in the plane H_i. The points marked with empty dots are orthogonal projections to H_i. An overview (left), and a detailed view around D_{i+1} (right).

We can use Taylor's estimate for the direction vectors $\beta'(t)$, as well. It yields

$$|\beta'(t) - \beta'(s)| \leq M\,|t - s|. \tag{3.11}$$

We are now ready to specify $\delta > 0$. Let

$$\delta = \frac{a}{10T} \min\left\{1, \frac{1}{M}\right\}. \tag{3.12}$$

In particular, note that

$$\delta \leq \frac{1}{10},\ \delta \leq \frac{a}{10T},\ \text{and}\ \delta \leq \frac{a}{10TM}.$$

The Taylor estimate (3.10) with $s = t_i$ and $t = t_{i+1}$ gives

$$\begin{aligned}
&|\beta(t_{i+1}) - (\beta(t_i) + (t_{i+1} - t_i)\beta'(t_i))| \leq \\
&\leq \frac{M}{2}(t_{i+1} - t_i)^2 \leq \frac{M}{2}\delta(t_{i+1} - t_i) \\
&\leq \frac{M}{2}\frac{a}{10MT}(t_{i+1} - t_i) \leq \frac{a}{20T}(t_{i+1} - t_i),
\end{aligned} \tag{3.13}$$

and (3.11) similarly gives

$$\begin{aligned}
|\beta'(t_{i+1}) - \beta'(t_i)| &\leq M(t_{i+1} - t_i) \leq M\delta \\
&\leq M\frac{a}{10TM} = \frac{a}{10T}.
\end{aligned} \tag{3.14}$$

Proof Lemma 3.1. (i) We show that $\beta(t_i)$ and h_i lie on opposite sides of the line $H_i \cap H_{i+1}$. Instead of computing $H_i \cap H_{i+1}$ explicitly, we approximate its location using $\gamma_{\rm left}(t_i)\gamma_{\rm right}(t_i)$ and the orthogonal projection of $\gamma_{\rm left}(t_{i+1})\gamma_{\rm right}(t_{i+1})$ to the plane H_i.

Assume that P stands on facet f_i for some $i \in \{1, \ldots, n-1\}$. The plane H_i contains facet f_i, line $\ell(t_i)$, segment $\gamma_{\rm left}(t_i)\gamma_{\rm right}(t_i)$, and its midpoint $\beta(t_i)$; refer to Figs. 4 and 5. The vertical projection of o to H_i is h_i. Recall that h_i lies in the plane $\langle\beta(t_i), \beta'(t_i)\rangle$, which is orthogonal to $\ell(t_i)$ (by definition). Therefore the segment $\beta(t_i)h_i$ is orthogonal to $\ell(t_i)$, and parallel to the vector $\beta'(t_i)$.

Next we approximate the orthogonal projection of $\gamma_{\rm left}(t_{i+1})\gamma_{\rm right}(t_{i+1})$ and its midpoint $\beta(t_{i+1})$ to H_i. From (3.13), $\beta(t_{i+1})$ lies in a ball of radius

$$r_{i+1} := \frac{a(t_{i+1} - t_i)}{20T}. \tag{3.15}$$

centered at

$$c_{i+1} := \beta(t_i) + (t_{i+1} - t_i)\beta'(t_i). \tag{3.16}$$

Denote this ball by D_{i+1}. Its center c_{i+1} is on the ray $\overrightarrow{\beta(t_i)h_i}$, and by (3.13) and (3.7) we have

$$\begin{aligned}
|\beta(t_i)c_{i+1}| &= |(t_{i+1} - t_i)\beta'(t_i)| \\
&\geq (t_{i+1} - t_i)(1 - a) \\
&\geq 0.9(t_{i+1} - t_i). \qquad (3.17)\\
|\beta(t_i)c_{i+1}| &= |(t_{i+1} - t_i)\beta'(t_i)| \\
&\leq (t_{i+1} - t_i) \cdot (1 + a/T) \\
&\leq \delta(1 + a/T) \\
&\leq (1 + a/T) \cdot \frac{a}{10T} \\
&\leq (1 + 0.1) \cdot \frac{a}{10T} < \frac{a}{9T}. \qquad (3.18)
\end{aligned}$$

By (3.8) and (3.18), we have

$$|\beta(t_i)h_i| \geq \frac{a}{3T} > \left(1 + \frac{a}{T}\right)\frac{a}{10T} \geq |\beta(t_i)c_{i+1}|.$$

It follows that c_{i+1} (the center of D_{i+1}) is on the line segment $\beta(t_i)h_i$.

The orthogonal projection of $\beta(t_{i+1})$ to H_i lies in the disk $H_i \cap D_{i+1}$. The direction vector of $\ell(t_i)$ is given by the cross product $\beta(t_i) \times \beta'(t_i)$; and the direction vector of $\ell(t_{i+1})$ is given by $\beta(t_{i+1}) \times \beta'(t_{i+1})$.

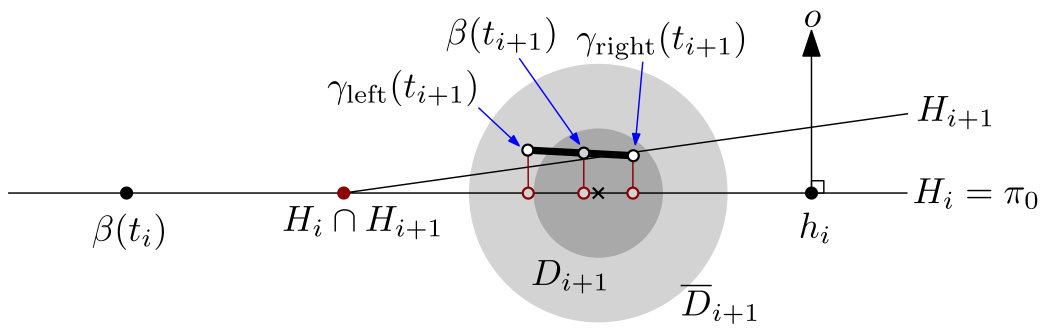

Figure 5: Points $\beta(t_i)$ and h_i in a plane perpendicular to $H_i \cap H_{i+1}$. The points marked with empty dots are orthogonal projections to this plane.

From (3.10) and (3.14), we have $|\beta'(t_i) - \beta'(t_{i+1})| \le a/10T$ and $|\beta(t_i) - \beta(t_{i+1})| \le (M/2)\delta^2 \le (a/T)^2/200$. This implies that the line $\ell(t_{i+1})$ is nearly parallel to $\ell(t_i)$, and so its orthogonal projection to H_i is also nearly parallel to it.

We may assume that the angle between $\ell(t_i)$ and the projection of $\ell(t_{i+1})$ is less than $\pi/4$. We would like to locate the intersection point of $\beta(t_i)h_i$ and the orthogonal projection of $\ell(t_{i+1})$ to H_i; denote this point by q_{i+1} Since $\beta(t_{i+1}) \in D_{i+1}$, the point q_{i+1} lies in the projection of the the disk $H_i \cap D_{i+1}$ to line $\beta(t_{i+1})h_i$, where the direction of the projection makes an angle at most $\pi/4$ with ℓ_{i+1} (i.e., an angle more than $\pi/4$ with $\beta(t_{i+1})h_i$); see Fig 4(right). In particular, either $q_{i+1} \in H_i \cap D_{i+1}$ or the tangents from q_{i+1} to the disk $H_i \cap D_{i+1}$ subtend an angle of at least $2(\pi/4) = \pi/2$. In both cases, q_{i+1} lies in a circumscribed square of $H_i \cap D_{i+1}$. Let D'_{i+1} be the ball concentric with D_{i+1} with radius $2r_{i+1}$. Then the projection of $\ell(t_{i+1})$ crosses $\beta(t_i)h_i$ in $H_i \cap D'_{i+1}$.

From (3.15) and (3.17) we obtain

$$2r_{i+1} = \frac{a(t_{i+1} - t_i)}{10T} \le 0.01(t_{i+1} - t_i)$$
$$< 0.9(t_{i+1} - t_i) \le |\beta(t_i)c_{i+1}|. \tag{3.19}$$

Further, from Equations (3.15), (3.12), and (3.8), we obtain

$$6r_{i+1} = \frac{3a(t_{i+1} - t_i)}{10T} \le \frac{3a\delta}{10T}$$
$$\le \frac{3a}{100T} < \frac{a}{3T} \le |\beta(t_i)h_i|. \tag{3.20}$$

Combined with (3.18) and (3.19) this yields

$$|c_{i+1}h_i| \ge |\beta(t_i)h_i| - |\beta(t_i)c_{i+1}|$$
$$\ge \frac{a}{3T} - \frac{a}{9T} = \frac{2a}{9T} > \frac{2a}{10T}$$
$$> \frac{2a}{10T}(t_{i+1} - t_i) = 4r_{i+1}. \tag{3.21}$$

Consequently, D'_{i+1} contains neither $\beta(t_i)$ nor h_i, that is, D'_{i+1} lies between $\beta(t_i)$ and h_i.

Since line $\ell_i := H_i \cap H_{i+1}$ separates f_i and the (orthogonal) projection of f_{i+1} to H_i, ℓ_i crosses the segment $\beta(t_i)h_i$ between $\beta(t_i)$ and the projection of $\gamma_{\text{left}}(t_{i+1})\gamma_{\text{right}}(t_{i+1})$, which lies in D'_{i+1}. Thus ℓ_i crosses the segment $\beta(t_i)h_i$ between $\beta(t_i)$ and h_i. As $\beta(t_i) \in \gamma_{\text{left}}(t_i)\gamma_{\text{right}}(t_i) \subset f_i$, we conclude that f_i and h_i lie on opposite sides of ℓ_i.

(ii) Assume that if P stands on face f_i for some $i \in \{1, \ldots, n-1\}$, it rolls to face f_j. Initially, the center of mass, $\xi(P)$, is at distance $|oh_i| < |\beta(t_i)| \le 1$ from the ground, and it can only move closer to the ground, hence $|h_j| < |h_i|$. The line $H_i \cap H_j$ must intersect B, otherwise the center of mass would be at distance more than 1 from the ground during the motion. Since $B' \subset P$, this further implies that $H_i \cap H_j$ intersects $B \setminus B'$.

Recall that $\partial B \cap \partial B'$ is a Jordan curve S_0 composed of γ_{left}, γ_{right}, and a halfcircle centered at $\beta(T)$; and the boundary $\partial(B \setminus B')$ is composed of two surface patches: a surface patch S_1 of $\partial B'$ that consists of the surface swept by the segment $\gamma_{\text{left}}(t)\gamma_{\text{right}}(t)$ for all $t \in [0, T]$ and a halfdisk centered at $\beta(T)$; and a surface patch S_2 of the sphere ∂B bounded by S_0. Refer to Fig. 3.

Consider now $P \cap (B \setminus B')$. Since $B' \subset P$, the boundary of $P \cap (B \setminus B')$ contains S_0 and S_1, but the surface patch S_2 is replaced by a surface patch S_3 of $P \cap B$ bounded by the Jordan curve S_0. The line segments $\gamma_{\text{left}}(t_k)\gamma_{\text{right}}(t_k)$, for $k = 2, \ldots, n$, each lie in both S_1 and S_3. Since these $n-1$ line segments are pairwise disjoint chords of the Jordan curve S_0, the deletion of these segments partitions $P \cap (B \setminus B')$ into n components, each of which is incident to at most two segments, $\gamma_{\text{left}}(t_k)\gamma_{\text{right}}(t_k)$ and $\gamma_{\text{left}}(t_{k+1})\gamma_{\text{right}}(t_{k+1})$ for some $k = 1, \ldots, n$. In particular, f_i has only two edges that intersect B, namely $f_i \cap f_{i-1}$ and $f_i \cap f_{i+1}$. Since $|h_{i-1}| > |h_i| > |h_{i+1}|$, the polytope cannot roll from f_i to f_{i-1}, consequently it rolls from f_i to f_{i+1}. □

Distance between initial and final footprints. We choose the arc γ to ensure that P covers a distance at least L when it successively rolls from face f_1 to f_n (i.e., the distance between the initial and final footprints is at least L).

Let C_0 be a great circle of B in the plane $x = 0$; and let C_1 and C_2 be two circles in ∂B that lie in two parallel planes $x = \frac{-1}{5L}$ and $x = \frac{1}{5L}$, respectively. The tangent lines to C_0 form a cylinder of radius 1; and the tangent lines to C_1 (resp., C_2) form a cone of aperture $2\arcsin(\frac{1}{5L})$. If B rolls once along C_0, its contact point with π_0 traces out a straight line segment of length $\text{len}(C_0) = 2\pi$; and similarly, if B rolls once along C_i, it traces out a circular arc of length $\text{len}(C_i)$ of the circle $\widehat{C}_i$ $(i = 1, 2)$ of radius $\sqrt{25L^2 - 1}$ centered at the apex of the cone of tangent lines.

We choose γ as a dense and long spiral that lies strictly between C_1 and C_2. Let $T = 4L$, and $\gamma : [0, 4L] \to \partial B$ be defined as follows:

(3.22)
$$x(t) = \frac{t - 2L}{10L^2},$$
$$\gamma(t) = \left(x(t), \cos(t)\sqrt{1 - x^2(t)}, \sin(t)\sqrt{1 - x^2(t)}\right).$$

A *loop* of γ is the image of an interval of length 2π in $[0, 4L]$. Note that (i) $-1/(5L) \le x(t) \le 1/(5L)$; and (ii) the x-coordinate of $\gamma(t)$, $x(t)$, increases by $2\pi/10L^2 > 1/(2L^2)$ after each loop. The arclength of every loop is at least $\text{len}(C_1) = 2\pi\sqrt{1 - 1/(5L)^2}$, and so the arclength of γ is at least $4L\sqrt{1 - 1/(5L)^2} > 3.9\,L$.

We re-parameterize γ by arclength, as the machinery introduced above for the general construction requires such a parameterization. Each loop of the spiral is close to the great circle $C_0 = \{(0, \cos t, \sin t) : t \in [0, 2\pi)\}$, which is parameterized by arclength and its first and second derivatives are unit vectors. After reparameterization, T equals the arclength of T, that is $T > 3.9\ L$, and M is close to 1, consequently we may assume that $M \le 2$.

Set $a = 1/(6400\ L^4)$; in particular $a \le 1/10$. We have $|\gamma_{\text{left}}(t)\gamma_{\text{right}}(t)| \le 4a^{1/2} = 1/(20L^2)$, for all $t \in [0, T]$. Since the x-coordinates of $\gamma(t)$ increase by more than $1/(2L^2)$ after each loop (regardless of the re-parameterization), γ_{left} and γ_{right} are disjoint simple arcs, and they both lie between C_1 and C_2. Recall that $\delta = \frac{a}{10T}\min\{1, 1/M\}$, thus $\delta = O(1/L^4 \cdot 1/L) = O(1/L^5)$. Since $T = \Theta(L)$, a subdivision of $[0, T]$ into intervals of length at most δ requires $\Theta(L^6)$ subdivision points; this yields $n = \Theta(L^6)$.

As P rolls through the faces $f_1, f_2, \ldots, f_n$, the points $\beta(t_i)$ $(i = 1, \ldots, n)$ are successively in contact with the horizontal plane π_0, and trace out a polygonal path $\Gamma = (p_1, p_2, \ldots, p_n) \subset \pi_0$. Alternatively, Γ is the development of the geodesic path $(\beta(t_1), \ldots, \beta(t_n))$ on ∂P. It remains to estimate the total length of Γ and the distance between its two endpoints.

We prove that $|p_1p_n| \ge 3.2L$, by establishing a lower bound $\text{len}(\Gamma) > 3.8\ L$, and then bounding the deviation of Γ from a straight-line path.

The portion of the geodesic path $(\beta(t_1), \ldots, \beta(t_n))$ on ∂P between $\beta(t_i)$ and $\beta(t_{i+1})$, for $i = 1, \ldots, n-1$, is a polygonal path contained in $f_i \cup f_{i+1}$, with a bend point at $f_i \cap f_{i+1}$. Recall that

$$\text{len}(\gamma) = \sum_{i=1}^{n-1} |\gamma(t_i)\gamma(t_{i+1})| \ge 4L\sqrt{1 - \frac{1}{(5L)^2}} > 3.9\,L.$$

It follows that

$$\begin{aligned}\text{len}(\Gamma) > \text{len}(\beta) &> \sum_{i=1}^{n-1} |\beta(t_i)\beta(t_{i+1})| \\ &> (1-a)\sum_{i=1}^{n-1} |\gamma(t_i)\gamma(t_{i+1})| \\ &= (1-a)\,\text{len}(\gamma) > (1-a)\,3.9\,L > 3.8\,L.\end{aligned}$$

Let $\widehat{\gamma} : [0, T] \to \pi_0$ be the development of γ as B continuously rolls on the plane π_0 with a contact point at $\gamma(t)$; similarly, let $\widehat{\beta} : [0, T] \to \pi_0$ be the development of β as the convex body B' rolls on the plane π_0 with a contact point at $\beta(t)$ for $t \in [0, T]$.

In general, for a continuous curve $\alpha : [0, T] \to \mathbb{R}^2$, the *turning angle* $\varphi(t)$ at $t \in [0, T]$ equals the angle between the direction vectors $\alpha'(0)$ and $\alpha'(t)$ modulo 2π. If α is parameterized by arclength, and its signed curvature is $\kappa : [0, T] \to \mathbb{R}$, then the turning angle at t can be computed as follows; see [23, Sec. 2.2].

(3.23)
$$\varphi(t) = \int_{s=0}^{t} \kappa(s)\, ds.$$

For example, the turning angle of a simple closed curve (parameterized counterclockwise) is 2π, and a turning angle of a circular arc of central angle θ is exactly θ. We use this machinery to approximate the turning angle of the polygonal path Γ.

Since γ lies between the circles C_1 and C_2, the curvature of $\widehat{\gamma}$ is less than that of $\widehat{C}_1$ and $\widehat{C}_2$, i.e., less than $1/\sqrt{(5L)^2 - 1} \approx 1/(5L)$. The curvature of $\widehat{\beta}$ is close to that of $\widehat{\gamma}$ at every $t \in [0, T]$: Since $\beta(t) = (1 - at/T)\gamma(t)$ and $|\gamma''(t)| \le 2$, Equation (3.6) yields

$$
\begin{aligned}
|\beta(t)-\gamma(t)| &= (at/T)|\gamma(t)| = at/T \le a,\\
|\beta'(t)-\gamma'(t)| &\le (at/T)|\gamma'(t)| + (a/T)|\gamma(t)|\\
&\le a + a/T \le 2a,\\
|\beta''(t)-\gamma''(t)| &\le (at/T)|\gamma''(t)| + 2(a/T)|\gamma'(t)|\\
&\le 2a + 2a/T \le 4a.
\end{aligned}
$$

While it would be tedious to compute the curvatures of $\widehat{\gamma}$ and $\widehat{\beta}$ exactly, the *curvature* of a curve can be expressed as a rational function of the coordinates of the curve itself and its first and second derivatives (in terms of cross products and determinants); see [25, Sec. 1.4]. It follows that the curvatures of $\widehat{\gamma}$ and $\widehat{\beta}$ differ by at most $O(a) = O(L^{-4})$. For sufficiently large $L > 0$, the curvature of $\widehat{\beta}$ is less than $1/(5L) + O(L^{-4}) < 1/(4L)$. Since $\text{len}(\widehat{\beta}) = \text{len}(\beta) < \text{len}(\gamma) < 4L$, Eq. (3.23) implies that the turning angle of $\widehat{\beta}$ does not exceed

$$\int_{s=0}^{4L} \frac{1}{4L}\, ds = 1 \le \frac{\pi}{3}.$$

Moreover, the turning angle of any subarc of $\widehat{\beta}$ is also bounded by $\pi/3$, and so all direction vectors $\widehat{\beta}'(t)$, $t \in [0, T]$, are in a cone of aperture at most $\pi/3$.

In the polygonal path $\Gamma = (p_1, p_2, \ldots, p_n)$, the turning angles $\angle(\overrightarrow{p_{i-1}p_i}, \overrightarrow{p_ip_{i+1}})$ are close to $\angle(\widehat{\beta}'(t_i), \widehat{\beta}(t_{i+1}))$ for $i = 2, \ldots, n-1$. Therefore, we may assume that the vectors $\overrightarrow{p_{i-1}p_i}$, $i = 1, \ldots, n-1$, are in a cone of aperture at most $\pi/3$. If ℓ is the angle bisector of this cone, ℓ makes an angle of at most $\pi/6$ with every edge of Γ. If $x_i > 0$ is the length of the projection of p_ip_{i+1} onto ℓ, we have $|p_ip_{i+1}| \le x_i/\cos(\pi/6)$, for $i = 1, \ldots, n-1$. Since $\sum_{i=1}^{n-1} x_i = |p_1p_n|$, this yields

$$
\begin{aligned}
\text{len}(\Gamma) &= \sum_{i=1}^{n-1} |p_ip_{i+1}| \le \sum_{i=1}^{n-1} \frac{x_i}{\cos(\pi/6)}\\
&\le \sum_{i=1}^{n-1} \frac{2}{\sqrt{3}} x_i = \frac{2}{\sqrt{3}} |p_1p_n| < 1.16\, |p_1p_n|.
\end{aligned}
$$

Consequently, $|p_1p_n| \ge \text{len}(\Gamma)/1.16 > 3.2\, L$, as claimed.

Unit diameter. If γ is chosen as in (3.22), then the normal vectors of the planes H_i, $i = 1, \ldots, n$, are nearly orthogonal to the x-axis, and the diameter of P might be quite large. To ensure that $\text{diam}(P) = 1$, we modify γ, by attaching two additional x-monotone spirals to each of its endpoints that lead to the points $(-1, 0, 0)$ and $(1, 0, 0)$ of ∂B, respectively. The length of these spirals is $\Theta(1)$, and the spirals could decrease the distance between the initial and final footprints by at most $O(1)$. See Fig. 6.

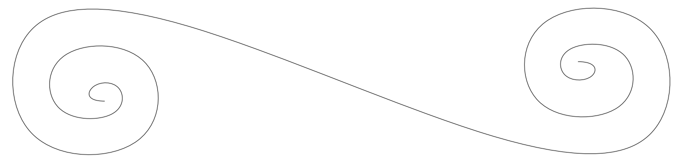

Figure 6: A bird's eye view of the polygonal path $\Gamma \in \pi_0$, the trail of a unistable polytope P whose flips cover a large distance.

Based on the choice of γ from (3.22) and moreover, due to the two spirals attached to its endpoints, P is bounded and its diameter is close to 1. Indeed, the normal vectors of the planes H_1 and H_n at the two endpoints $\beta(t_1)$ and $\beta(t_n)$ are nearly parallel to the x-axis, consequently $\text{diam}(P) \lessapprox 2\sqrt{2} < 3$. A suitable scaling by a ratio

$$\varrho = \frac{1}{\text{diam}(P)} \in \left(\frac{1}{3}, 1\right]$$

produces a polytope of unit diameter. The scaling preserves unistability and Hamiltonicity, while the distance between the initial and final footprints only decreases by a factor of ϱ; this distance is at least $\varrho\, 3.2\, L > \frac{1}{3}\, 3.2\, L > L$, as required. ∎

4 Other Variants of Rolling Polytopes

In this section, we prove that a Hamiltonian unistable polytope can be an arbitrarily close approximation of a ball. For $\varepsilon > 0$, a polytope P is an ε-*approximation* of the unit ball B if $(1-\varepsilon)B \subset P \subset (1+\varepsilon)B$.

Theorem 4.1. *For every $\varepsilon > 0$, there is a Hamiltonian unistable (nonuniform) polytope P that ε-approximates the unit ball B while retaining the arbitrarily large rolling distance property. (The polytope P need not be uniform.)*

Proof. Let $\varepsilon \in (0, \pi/2)$ be given. We use the construction from the proof of Theorem 3.1 with a suitable arc $\gamma : [0, T] \to \partial B$, and parameter $a > 0$. First note that if $Q \subseteq \partial B$ is a finite set such that the spherical caps of radius ε centered at points in Q cover ∂B, then the planes tangent to B at the points in Q define a polytope P that satisfies the inclusions $B \subset P \subset (1+\varepsilon)B$.

Lay down a raster of circles in ∂B that lie in planes orthogonal to the x-axis such that the spherical distance between two consecutive circles is less than $\varepsilon/2$. Since the spherical distance between two antipodal points, $(-1, 0, 0)$ and $(1, 0, 0)$, is π, we use $2\lceil \pi/\varepsilon \rceil - 1$ circles.

Let $\gamma : [0, T] \to \partial B$ be a spiral from $(-1, 0, 0)$ to $(1, 0, 0)$ that makes one full rotation about the x-axis between consecutive raster circles. Then every point in

∂B lies between two raster circles, and is within distance $\varepsilon/2$ from some point on γ. We choose a subdivision $0 = s_1 < s_2 < \ldots < s_m = T$ such that the point set $Q = \{\gamma(s_i) : i = 1, \ldots, n\}$ defines a covering of ∂B by spherical caps of radius ε.

Next, choose a sufficiently small $a \in (0, \varepsilon/2)$ such that the polytope $P_0 = \bigcap_{i=1}^{m} H(s_i)^+$ lies in $(1+\varepsilon)B$, where the halfspaces H_i, $i = 1, \ldots, n$ are defined for the curve $\beta(t) = (1 - at/T)\gamma(t)$ as in the proof of Theorem 3.1. Finally, refine the subdivision $0 = s_1 < s_2 < \ldots < s_m = T$ into a subdivision $0 = t_1 < t_2 < \ldots < t_n = T$, if necessary, to meet all constraints of that construction. None of the additional tangent planes $H(t_i)$, $i = 1, \ldots, n$, intersects $(1-\varepsilon)B$. Consequently, the polytope $P_1 = \bigcap_{i=1}^{n} H(t_i)^+$ contains $(1-\varepsilon)B$, and is contained in $(1+\varepsilon)B$, as required. □

Uniform density. A variant of the polytope in Theorem 3.1 can be constructed from material of uniform density.

THEOREM 4.2. *For every $L \geq 1$, there exits a uniform polytope P of unit diameter and a facet f_1 such that if P stands on face f_1 it rolls to distance at least L. (The polytope P need not be unistable or Hamiltonian.)*

Proof. We start with a uniform unit ball B centered at the origin $\mathbf{0}$ and let $\varepsilon \in (0, 0.01)$ be sufficiently small as specified below. By Theorem 4.1, there is a nonuniform unistable Hamiltonian polytope $P = P(L, \varepsilon)$ that ε-approximates B, and P has a sequence of facets $f_1, \ldots, f_n$ that all lie in the slab between the parallel planes $x = -1/(5L)$ and $x = 1/(5L)$ such that if P stands on facet f_i $(i = 1, \ldots, n-1)$, it rolls to face f_{i+1}, and the distance between the footprints at f_1 and f_n is at least L.

However, unlike in construction in the proofs of Theorem 3.1 and Theorem 4.1, the faces of P outside of the parallel slab between $x = -1/(5L)$ and $x = 1/(5L)$ lie in the exterior of B; i.e., we do not use the any spirals from $(-1, 0, 0)$ to $(1, 0, 0)$. In particular, P never rolls to any of these faces from the faces $f_1, \ldots, f_n$, and so P is neither unistable nor Hamiltonian.

Note that neither B nor P contains the other body. The volume of the symmetric difference of B and P is bounded above by $\frac{4\pi}{3}[(1+\varepsilon)^3 - (1-\varepsilon)^3] = O(\varepsilon)$. Consequently, the center of mass $\xi(P)$ shifts by $O(\varepsilon)$ as well, i.e., $\xi(P)$ lies in a ball of radius $O(\varepsilon)$ centered at $\mathbf{0}$.

To move the center of mass of P back to the origin we first determine four points $q_1, q_2, q_3, q_4 \in \partial P$ so that the tetrahedron $\Delta = \mathrm{conv}(q_1, q_2, q_3, q_4)$ closely approximates a regular tetrahedron inscribed in B, and they are each at distance at least $1/3$ from the plank between $x = \pm 1/(5L)$. We now stack four "mountains" above the points q_1, q_2, q_3, q_4 by raising the four points and updating the convex hull. Specifically, we construct $P' = \mathrm{conv}(P, q_1', q_2', q_3', q_4')$, where q_i' is a mountain top, and $oq_i \subseteq oq_i'$, for $i = 1, \ldots, 4$. The heights of the mountains (i.e., $h_i = |oq_i'|$ for $i = 1, \ldots, 4$) are variables that we can set so as to annihilate the shift of the center of mass in the opposite direction. The volume of each mountain monotonically increases with its height, and is concentrated to a neighborhood of radius at most $\sqrt{h_i^2 - (1-\varepsilon)^2}$. If $h_i \leq 1.105 < \sqrt{10/9}$, then this radius is less than $1/3$, and the mountain at q_i is disjoint from all faces $f_1, \ldots, f_n$. Each coordinate of the center of mass $\xi(P')$ is a piecewise rational function of the heights h_i $(i = 1, \ldots, 4)$. If we set $h_1 = 1.05$ and $q_i' = q_i$ for $i = 2, 3, 4$, then $\xi(P')$ shifts roughly towards q_i by a small constant (independent of ε). Provided that $\varepsilon > 0$ is sufficiently small, by the (multidimensional) intermediate value theorem, there exit suitable heights $h_i \in [1-\varepsilon, 1.1]$, $i = 1, \ldots, 4$, for which $\xi(P')$ is the origin. □

5 Concluding Remarks

We suspect that the properties in Theorems 4.1 and 4.2 can be combined; we leave this as an open problem: Is there a Hamiltonian unistable uniform polytope of unit diameter that can roll to an arbitrary given distance away?

The perpetuum mobile desideratum. We know (by Lemma 1.2) that no polytope exists that can roll on forever; indeed, this is so because every polytope has a finite number of faces. This leaves open the existence of a (smooth) convex body that can roll on forever. While we cannot rule out this possibility, we can immediately observe that our construction method (i.e., scraping off a neighborhood of a spherical arc from a ball) is due to fail: Indeed, the width of the neighborhood of the arc γ is positive and strictly increasing, and by construction, this thickened arc cannot cross itself. As such, if γ were an infinite arc, then this neighborhood would also have infinite area, contradicting the fact that the surface area of the ball is bounded.

Diameter versus girth. Conway [16] (see also [7, Sec. B12]) constructed a convex unistable polytope whose diameter to girth ratio is at most $3/\pi + \varepsilon$, for any $\varepsilon > 0$. He also asked: What is the smallest possible diameter to girth ratio for a convex unistable polyhedron? (The *girth* is the minimum length of the perimeter of a projection onto a plane.) Our construction (Theorem 4.1) shows that a ratio of $1/\pi + \varepsilon$, for any $\varepsilon > 0$, can be attained with nonuniform polytopes.

Trajectories for programmable robots. What can be said about the class of planar trajectories that can be generated by this mechanism? More precisely, what properties can be established for the contact curves when gravity rolls a smooth convex body in $\mathbb{R}^3$ on a horizontal plane? The arc γ drawn on a ball B (as well as β on the smooth body B') is noncrossing, however, it is unclear whether the corresponding planar trajectory $\zeta(\gamma)$ crosses itself. Is the set of possible trajectories $\zeta(\gamma)$ obtained in this way dense in the set of all continuous arcs in the plane? It is known for instance that *closed convex curves* and *slice curves* drawn on convex polytopes develop without self-intersection [19, 20]; see also [21].

Our method for designing unistable polytopes could perhaps be used to obtain *programmable* robotic modules, whose trajectories are written in advance by drawing suitable curves on the raw balls. Obviously the programs can be different and so group formations with different motion plans can be handled for independent and/or simultaneous movement, provided that collisions can be avoided. See for instance advances in chemistry and physics in the last two decades in the area of hydraulic design at a molecular scale [1, 4, 22, 27].

References

[1] John M. Abendroth, Oleksandr S. Bushuyev, Paul S. Weiss, and Christopher J. Barrett, Controlling motion at the nanoscale: Rise of the molecular machines, *ACS Nano* **9(8)** (2015), 7746–7768, `doi:10.1021/acsnano.5b03367`.

[2] Vladimir I. Arnold, *Ordinary Differential Equations*, 10th printing, MIT Press, Cambridge, MA, 1998.

[3] András Bezdek, On stability of polyhedra, in: *Workshop on Discrete Geometry (Sep 13–16, 2011)*, Fields Institute, Toronto, ON, 2011, pp. 2490–2491.

[4] Richard A. Bissell, Emilio Córdova, Angel E. Kaifer, and J. Fraser Stoddart, A chemically and electrochemically switchable molecular shuttle, *Nature* **369** (1994), 133-137.

[5] Sergey A. Chaplygin, On a sphere rolling on a horizontal plane (in Russian), *Mathematical Collection of the Moscow Mathematical Society* **24** (1903), 139–168. An English translation appeared in *Regular and Chaotic Dynamics* **7(2)** (2002) 131–148.

[6] John H. Conway and Richard K. Guy, Stability of polyhedra, *SIAM Review* **8(3)** (1966), p. 381.

[7] Hallard T. Croft, Kenneth Falconer, and Richard K. Guy, *Unsolved Problems in Geometry*, Springer, New York, NY, 1991.

[8] Robert J. MacG. Dawson, Monostatic simplexes, *The American Mathematical Monthly* **92(8)** (1985), 541–546.

[9] Robert J. MacG. Dawson and Wendy Finbow, What shape is a loaded die? *Mathematical Intelligencer* **21(2)** (1999), 32–37.

[10] Robert J. MacG. Dawson, Wendy Finbow, and Philip Mak, Monostatic simplexes II, *Geometriae Dedicata* **70(2)** (1998), 209-219.

[11] Robert J. MacG. Dawson and Wendy Finbow, Monostatic simplexes III, *Geometriae Dedicata* **84(1-3)** (2001), 101-113.

[12] Gábor Domokos, Flórián Kovács, Zsolt Lángi, Krisztina Regős, and Péter T. Varga, Balancing polyhedra, preprint, arxiv:1810.05382, 2018.

[13] Gábor Domokos, Zsolt Lángi, and Tímea Szabó, A topological classification of convex bodies, *Geometriae Dedicata* **182** (2016), 95–116.

[14] Gábor Domokos, Zsolt Lángi, and Tímea Szabó, On the equilibria of finely discretized curves and surfaces, *Monatsh. Math.* **168** (2012), 321–345.

[15] Carl Friedrich Gauss, Über ein neues allgemeines Grundgesetz der Mechanik, *J. reine angew. Math. (Crelles Journal)* **4** (1829), 232–235.

[16] Michael Goldberg and Richard K. Guy, Stability of polyhedra (J. H. Conway and R. K. Guy), *SIAM Review* **11(1)** (1969), 78–82.

[17] Richard K. Guy, Twenty odd questions in combinatorics, in *Combinatorial Mathematics and its Applications*, R. C. Bose et al., editors, Chapel Hill, NC, 1970, pp. 209–237.

[18] Aladár Heppes, A double tipping tetrahedron, *SIAM Review* **9(3)** (1967), 599–600.

[19] Joseph O'Rourke, On the development of the intersection of a plane with a polytope, *Computational Geometry: Theory and Applications* **24(1)** (2003), 3–10.

[20] Joseph O'Rourke and Catherine Schevon, On the development of closed convex curves on 3-polytopes, *Journal of Geometry* **13** (1989), 152–157.

[21] Joseph O'Rourke and Costin Vîlcu, Development of curves on polyhedra via conical existence, *Computational Geometry: Theory and Applications* **47(2)** (2014), 149–163.

[22] Mark Peplow, The tiniest lego: A tale of nanoscale motors, rotors, switches and pumps, *Nature* **525** (2015), 18-21.

[23] Andrew Pressley, *Elementary Differential Geometry*, Springer, London, 2001.

[24] Alexander Reshetov, A unistable polyhedron with 14 faces, *Int. J. Comput. Geometry Appl.* **24(1)** (2014), 39–60.

[25] Dirk J. Struik, *Lectures on Classical Differential Geometry*, Addison- Wesley, Reading, MA, 1961.

[26] Péter L. Várkonyi and Gábor Domokos, Static equilibria of rigid bodies: Dice, pebbles and the Poincaré-Hopf Theorem, *J. Nonlinear Sci.* **16** (2006), 255–281.

[27] Molecular machines (scientific background on the Nobel Prize in Chemistry 2016 prepared by The Royal Swedish Academy of Sciences); `https://www.nobelprize.org/uploads/2018/06/advanced-chemistryprize2016-1.pdf`